Peony Flower Polypeptides: A New Naturally Derived Bioactive Ingredient for Anti-Aging and Anti-Hair Loss Applications

Xinyi Chen[1], Benyue Li[1], Huaqian Mei[1], Jie Yang[1], Fengwei Qi[1]
[1]Shandong Huawutang Biological Technology Co., Ltd, Shandong, China

Abstract

This study aimed to evaluate the anti-aging and scalp care efficacy of peony flower polypeptides (PFP), a natural bioactive compound, through in vitro experiments and human scalp physiological analysis. The research explored the potential of PFP to improve skin and scalp health by examining its effects on cutaneous aging processes, scalp lipid metabolism, and female pattern hair loss. Experimental approaches included cytotoxicity testing, antioxidant assays, evaluation of collagen synthesis, measurement of hyaluronic acid and chondroitin sulfate content, and assessment of barrier repair proteins in cell models. Additionally, a cross-sectional study involving 240 female participants was conducted to analyze scalp physiological parameters and lipid metabolomics using UPLC-MS/MS technology combined with OPLS-DA modeling. The results demonstrated that PFP significantly inhibited acetylcholine and MMP-1 levels, enhanced collagen I and III expression, reduced UV-induced ROS production, and improved skin barrier integrity by increasing CLDN-1 and DSG1 expression. Scalp analysis revealed differences in physiological indicators and lipid profiles between hair loss and healthy populations, with differential metabolites enriched in sphingolipid and neurotrophin signaling pathways. In conclusion, PFP exhibited multi-targeted anti-aging and scalp care properties, providing a promising natural ingredient for future skincare and haircare formulations aimed at addressing skin aging, scalp aging, and hair loss.

Keywords: Peony flower polypeptides; Anti-aging; Scalp care; Hair loss; Bioactive peptides

1 Introduction

In modern bioscience and dermatological research, the exploration of natural, efficacious, and innovative bioactive compounds remains a pivotal area of interest. With the increasing societal focus on quality of life and aesthetics, the aging of cutaneous and scalp tissues has garnered heightened attention. Diminished elasticity, wrinkle formation, and alopecia have become significant dermatological concerns. Natural bioactive peptides, known for their potent efficacy and safety profiles, have been extensively investigated and applied in skincare and haircare products. Peony, a botanically and culturally significant plant, has attracted research interest due to its abundant bioactive constituents. Peony polypeptides (PFP) have demonstrated potential in promoting skin health because of their distinctive chemical structures and biological functionalities[1]. Recent studies have examined the efficacy of PFP in attenuating skin aging and mitigating hair loss. Utilizing advanced methodologies, researchers have explored the effects of PFP on critical physiological processes, including keratinocyte proliferation, collagen biosynthesis, antioxidant enzyme activity, and the regulation of hair follicle cycling. Accordingly, the investigation of PFP not only provides novel therapeutic avenues for skin and scalp health but also contributes to the development of innovative applications of natural bioactive agents in cosmetic and dermatological sciences[2]. Thus, this study rigorously explores the anti-aging and scalp care potential of PFP, offering substantial scientific merit and prospective translational value.

2 Experimental

2.1 Materials

Peony polypeptides (PFP, lab-made), MTT (Sigma), DMSO (Sigma), WY14643 (Sigma), SLS (Sigma), Paraformaldehyde (Biosharp), Claudin-1 antibody (Abcam), DSG1 antibody (Thermo Fisher), PBS (Vivacell, Gibco), Trypsin (Gibco), TGF-β_1 (peproTech), DCFH-DA (MCE), COL Ⅰ antibody (abcam), COLⅢ antibody (abcam), DAPI (Invitrogen), Claudin-1 ELISA kit (Enzyme-linked), DSG1 ELISA kit (Enzyme-linked), In Situ β-galactosidase Staining Kit (Beyotime), and Superoxide Assay Kit (Beyotime) were used in the study.

2.2 Instrumentation

The instruments used included an enzyme-linked immunosorbent assay (ELISA) system (BOIBASE), an incubator (HERAcell 150i, BLUEPARD), a biological cleanroom (LAYTE), a benchtop centrifuge (KECHENG), a water bath (AOHUA), a multimode microplate reader (Varioskan LUX), a quantitative real-time PCR system (ViiA-7), a gel imaging system (LIUYI), an electrophoresis system (LIUYI), a fluorescence microscope (Olympus, BX43,), an inverted microscope (Olympus, CKX53), a skin elasticity analysis system (Cutometer MPA580), Derma TOP-V3 (EO-TECH), and an inverted fluorescence microscope (BZ-X810).

2.3 Methods

2.3.1 Cytotoxicity Detection

When the percentage of resuscitated cells reached 60%, the cells were seeded into 96-well plates and incubated overnight in a CO_2 incubator (Thermo, 150I). After 24 h culture according to the designed concentration,s the supernatant was discarded, and the corresponding reagent was added. The optical density (OD) of each group was measured after incubation for 4 h.

2.3.2 In Vitro Test Methods

The contents of hyaluronic acid and chondroitin sulfate were detected using corresponding hyaluronic acid detection kits and chondroitin sulfate detection kits in the full-layer skin model. The levels of compact junction proteins and desmosomal core proteins were assessed through ELISA and immunofluorescence staining, allowing for the observation and quantitative analysis of target substances under a microscope. The acetylcholine content in the supernatant of the neuronal cell culture medium was detected using an acetylcholine detection kit. Following DCFH-DA staining of fibroblasts (Fbs), changes in intracellular reactive oxygen species (ROS) content were observed under a fluorescence microscope, and the average fluorescence intensity was calculated using ImageJ software to evaluate antioxidant efficacy. Immunofluorescence staining was also used to detect the expression of COL I and COL III in Fbs cells, with the average fluorescence intensity calculated using Image J software. For the color development method, working liquid samples with different concentrations were prepared according to the set concentrations, drugs were added, and culture was continued for 24 h. Testing and analysis were conducted according to the kit instructions. In the chemical staining method, 1 mL of medium containing samples at different concentrations was added based in the experimental design, and the samples were stained according to the manufacturer’s instructions.

2.3.3 Research on Female Pattern Hair Loss

This study included 120 Chinese female participants with hair loss and oily hair, along with 120 female participants with healthy scalps. The subjects were aged between 18 and 35

years, with body mass index (BMI) values ranging from 15.0 to 26.7. The selection criteria for participants with hair loss included excessive scalp oil, excessive hair loss, and hair loss counts greater than 10 out from 60 combing methods. Participants who were pregnant or breastfeeding, intended to become pregnant during the trial period, had received hair care or hair treatment within the last month, had dyed or permed their hair within the last month, had a BMI greater than 27, or had undergone hair transplantation or scalp disease treatment were excluded. This study followed the principles of the Declaration of Helsinki and the Good Clinical Practice (GCP) regulations. The research protocol was approved by the Shanghai Clinical Research Ethics Committee on December 26, 2023. All participants provided written informed consent[3].

The research design was a cross-sectional face-to-face study based on human trial data and questionnaire surveys. For experimental purposes, participants were instructed not to wash their hair within 48 ± 4 h before each scalp collection and not to comb their hair on the day of collection. They were required to comb their hair symmetrically on both sides to keep it smooth, maintaining the same hairstyle each time. Before the measurements, the subjects were required to wait for 30 min in a constant-temperature and constant-humidity environment. The participants were divided into four groups based on their scalp condition and geographical location, with experimental and control groups in Hangzhou and Beijing, respectively. Scalp physiological indicators and lipids were collected from the subjects.

3 Results and Discussion

3.1 Research Data on Female Pattern Hair Loss

By analyzing data on different scalp physiological indicators, significant differences were observed in skin pH, skin oil content, hair density, and hair loss count between the problem group and the normal population in both Hangzhou and Beijing (Figure 1). In particular, the moisture content of the stratum corneum in Hangzhou and the transepidermal water loss (TEWL) in Beijing showed significant differences between the two populations (Figure 1). These findings indicated that scalp oiliness, moisture retention capacity, and hair density were all closely associated with hair loss problems.

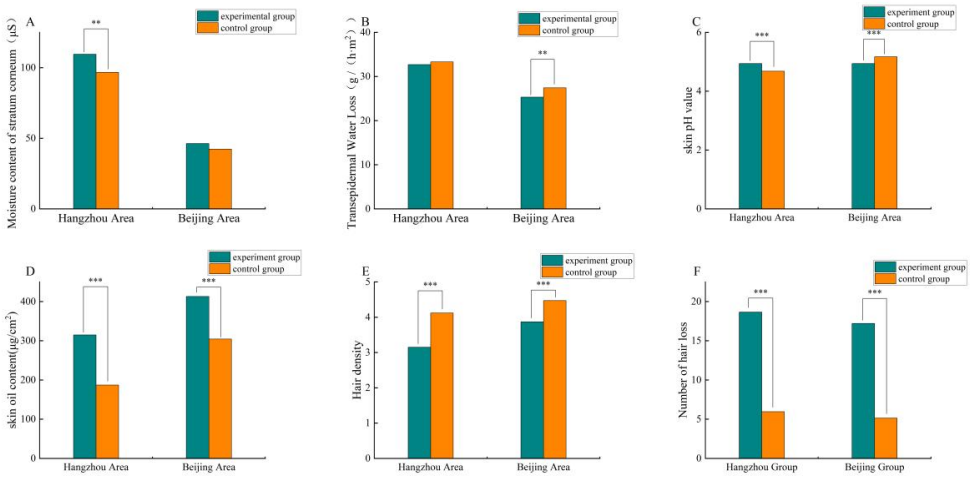

Figure 1. Physiological index data of the scalp. (A) The average moisture content of the stratum corneum of participants in Hangzhou and Beijing. (B) The average TEWL values of participants in Hangzhou and Beijing. (C) The average skin pH values of participants in

Hangzhou and Beijing. (D) The average skin oil content of participants in Hangzhou and Beijing. (E) The average hair density of participants in Hangzhou and Beijing. (F) The average hair loss count of participants in Hangzhou and Beijing. *** $p < 0.001$; ** $p < 0.01$; * $p < 0.05$.

Further investigation into the differences in scalp lipids between the problem and normal populations was conducted using an ultra-performance liquid chromatography-mass spectrometry-tandem mass spectrometry (UPLC-MS/MS) assay platform with extensive targeted metabolomics technology, which detected a total of 676 lipids in the subject samples. Orthogonal Partial Least Squares Discriminant Analysis (OPLS-DA) was employed to distinguish groups based on their metabolic profiles. This multivariate statistical analysis method, using supervised pattern recognition, effectively eliminated influences unrelated to the study and screened for different metabolites. After normalizing the scalp lipid data from both Beijing and Hangzhou, an OPLS-DA model was constructed. The scores for the Hangzhou experimental group (WT-HZ), Hangzhou control group (ZC-HZ), Beijing experimental group (WT-BJ), and Beijing normal group (ZC-BJ) were plotted in a paired analysis. The predictive ability of the model was evaluated using Q^2, which exceeded 0.5 for all control group comparisons (WT-BJ vs. ZC-BJ and WT-HZ vs. ZC-HZ) (Figure 2), indicating that the model construction was effective. The OPLS-DA scoring plot showed a clear separation between the different control groups (Figure 2).

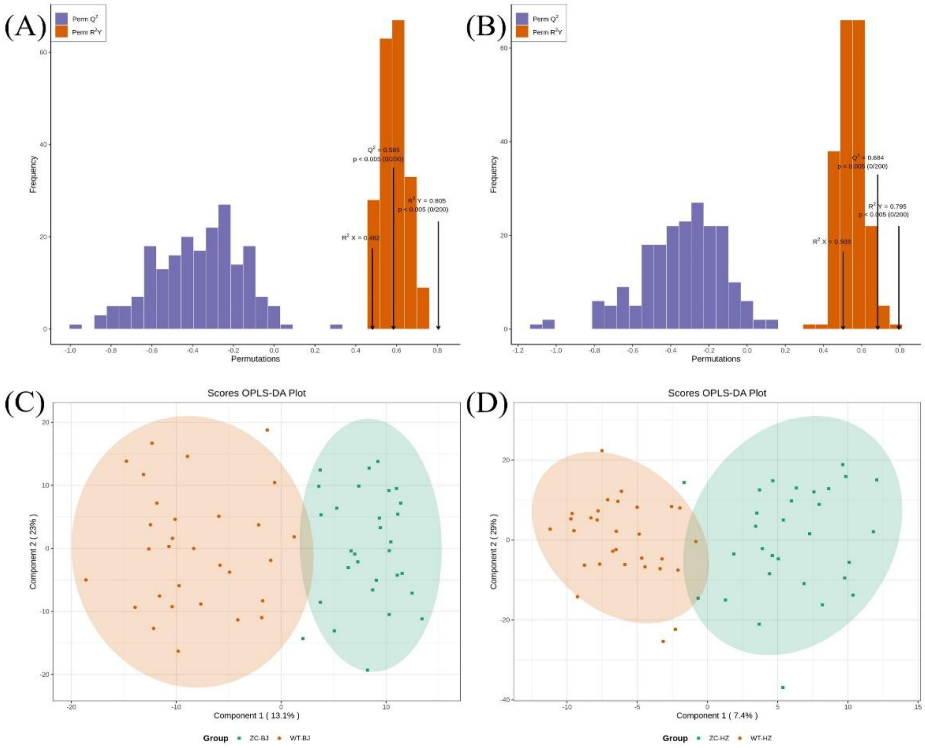

Figure 2. (A) OPLS-DA model validation plot for WT-BJ and ZC-BJ groups. (B) OPLS-DA model validation plot for WT-HZ and ZC-HZ groups. (C) OPLS-DA score plot for WT-BJ and ZC-BJ groups. (D) OPLS-DA score plot for WT-HZ and ZC-HZ groups.

Differential metabolites were screened based on fold change, variable importance in projection (VIP), and p-values. Lipid metabolites meeting the criteria of FC > 1.8, VIP > 1, and p-value < 0.05 were considered differential metabolites. The results showed that there were 83 differential metabolites between the WT-BJ and ZC-BJ groups, with 62 metabolites upregulated and 21 downregulated. Between the WT-HZ and ZC-HZ groups, there were 20 differential metabolites, with two upregulated and 18 downregulated (Figure 3).

All differential metabolites were matched with the KEGG database to obtain pathway information, and enrichment analysis was performed on the annotation results to obtain pathways with more enriched differential metabolites. The differential metabolites between the WT-BJ and ZC-BJ groups were mainly enriched in the sphingolipid metabolism, neurotrophin signaling, and adipocyte cytokine signaling pathways. Meanwhile, the differential metabolites between the WT-HZ and ZC-HZ groups were enriched in the sphingolipid metabolism, phosphatidylinositol metabolism, and ether lipid metabolism pathways[4]. Notably, certain metabolic pathways such as the sphingolipid metabolic pathway overlapped among all control group comparisons (Figure 3).

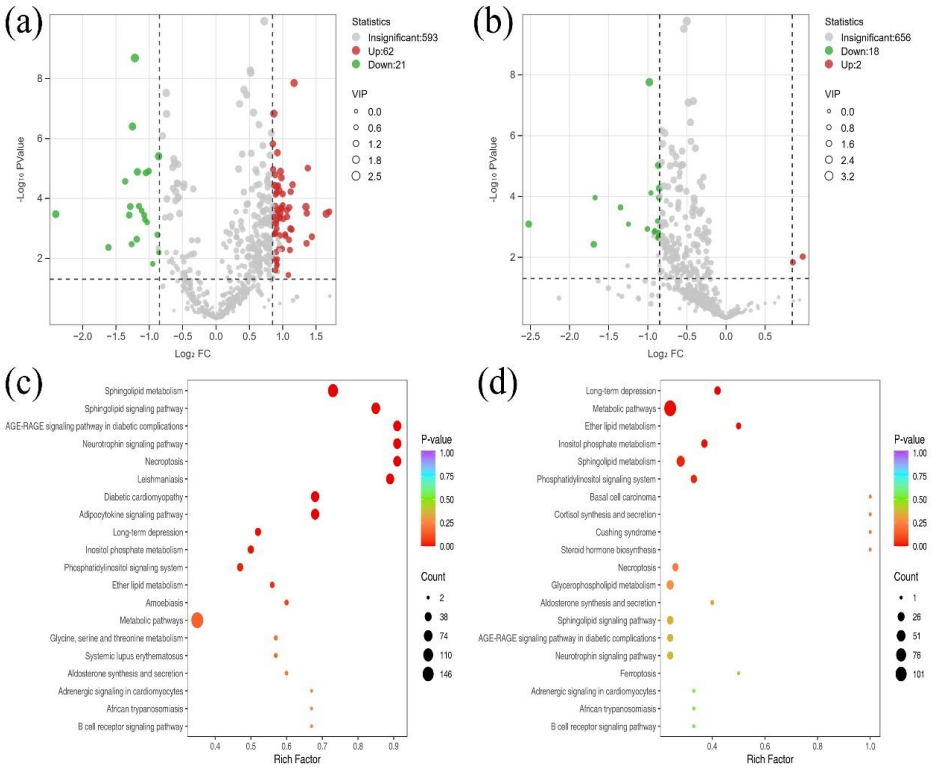

Figure 3. (A) Volcano plot of differential metabolites between WT-BJ and ZC-BJ groups. (B) Volcano plot of differential metabolites between WT-HZ and ZC-HZ groups. (C) Enrichment map of differential lipid pathways between WT-BJ and ZC-BJ groups. (D) Enrichment map of differential lipid pathways between WT-HZ and ZC-HZ groups.

3.2 Anti-aging Effect of PFP

3.2.1 In Vitro Anti-Aging Tests

In addition to its effects on HaCAT cells, the inhibitory effects of PFP on acetylcholine content in neuronal cells were examined. PFP showed no significant cytotoxicity on neurons within the concentration range of 0.01% to 0.002%. Compared with the blank control group,

PFP at concentrations of 0.05%, 0.01%, 0.005%, and 0.001% (w/v) significantly inhibited acetylcholine content ($p < 0.01$), with inhibition rates of 13.5% ± 0.2%, 12.8% ± 0.1%, 11.8% ± 0.2%, and 10.6% ± 0.2%, respectively. Moranin, a reference substance, inhibited acetylcholine, a neurotransmitter involved in muscle contraction and wrinkle formation, leading to muscle relaxation and anti-wrinkle effects.

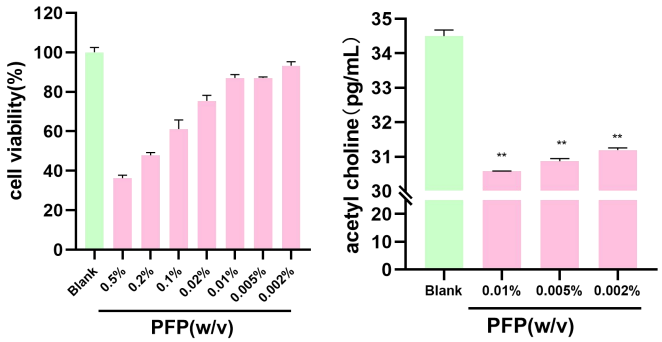

Figure 4. Effects of PFP on cytotoxicity in HaCAT cells and inhibition of acetylcholine content.

Further evaluation of PFP was conducted on its ability to mitigate ultraviolet (UV)-induced light damage. UV radiation is a primary cause of skin aging, leading to increased production of ROS and matrix metalloproteinase-1 (MMP-1) in the skin, which degrade collagen. Human skin-derived primary fibroblasts (Fbs) were used to study PFP's resistance to UV damage. Compared with the UV irradiation group (NC), the ROS inhibition rates of PFP at concentrations of 0.02%, 0.01%, and 0.001% (w/v) were 84.4% ± 0.2%, 83.1% ± 0.1%, and 82.4% ± 0.2%, respectively. The inhibition rates of MMP-1 were 99.5% ± 0.1%, 97.6% ± 0.2%, and 87.7% ± 0.1%, respectively.

In terms of collagen degradation induced by UV, PFP increased the expression of COL I to 69.0% ± 10.7%, 49.2% ± 7.6%, and 36.7% ± 7.3% at the same concentrations, and increased COL III expression to57.5% ± 16.5%, 53.2% ± 4.7%, and 36.8% ± 2.0%, respectively. Additionally, UV exposure affects the content of hyaluronic acid and chondroitin sulfate in the deep skin. Using the Skinovo®-Epi model, PFP showed no effect on cell activity within the range of 0.05%~1%. However, 0.05% (w/v) PFP significantly increased the content of hyaluronic acid and chondroitin sulfate, with increases of 18.25% ± 2.75% and 7.23% ± 4.19%, respectively ($p < 0.05$).

Hyaluronic acid plays a key role in moisturizing the skin and maintaining its elasticity and firmness[5], whereas chondroitin sulfate contributes to skin elasticity and regulates water balance[6]. The observed increase in the content of both components suggests that morantide may exert firming and anti-wrinkle effects by modulating the composition of the skin'sextracellular matrix.

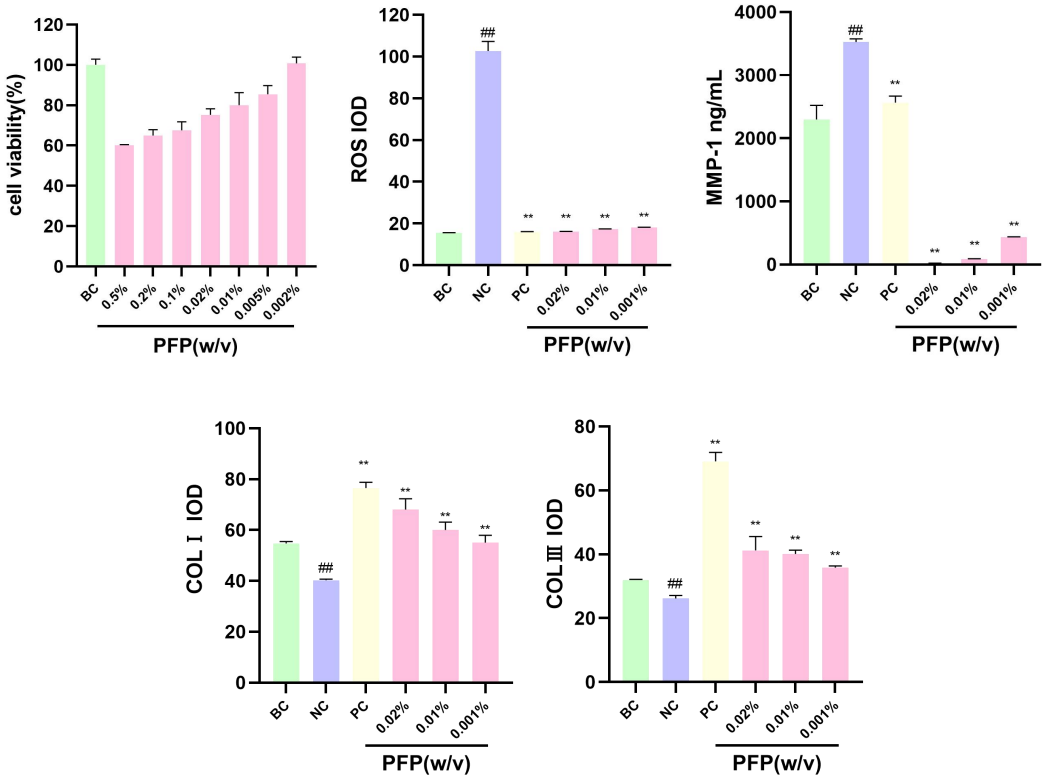

Figure 5. Cytotoxic effects of PFP on fibroblasts, inhibition of ROS production, and regulation of MMP-1, COL Ⅰ, and COLⅢ protein expression.

3.2.2 Repair of Skin Barrier Damage

Skin barrier function is crucial for preventing external environmental factors from invading the skin and accelerating skin aging[7]. Dense connexin 1 (CLDN-1) and desmosomal core 1 (DSG1) are key components in maintaining the function and structural integrity of the skin barrier. The results showed that 0.05% (w/v) PFP significantly increased the content of CLDN-1 and DSG1. The increase rates of CLDN-1 protein expression were 34.51% (ELISA) and 78.95% (immunofluorescence), whereas the increase rate of DSG1 protein expression was 103.13% (immunofluorescence).

These findings suggest that the increased content of these components indicates that morantide may contribute to repairing the damaged skin barrier and thereby exert a skin-repairing effect.

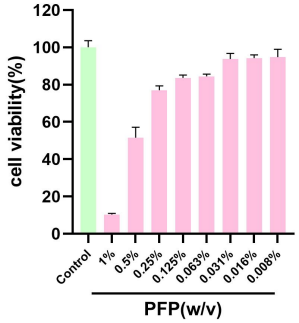

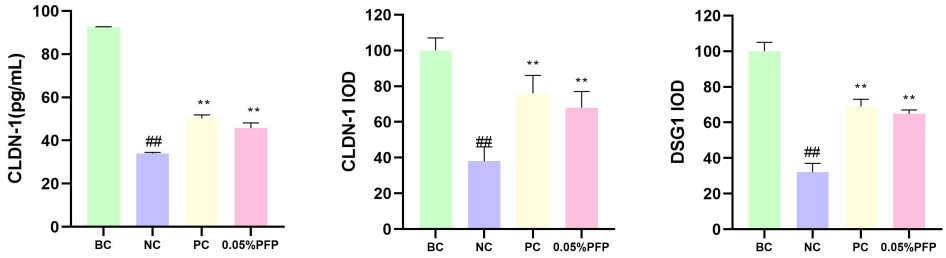

Figure 6. Regulation of barrier-associated proteins by PFP.

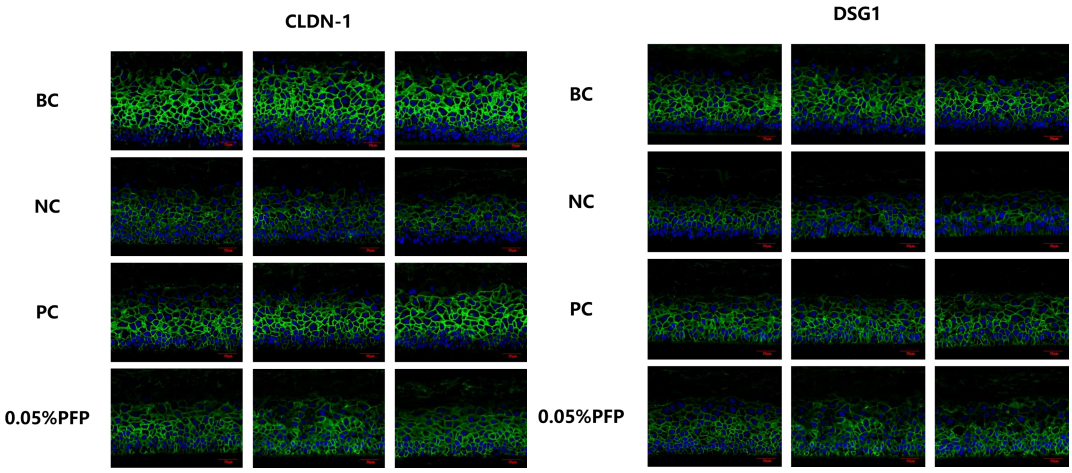

Figure 7. Immunofluorescence staining results for target proteins.

3.2.3 Scalp Anti-aging and Anti-Hair Loss Effects

Scalp aging is also an area of growing concern[8]. In the comparative study of scalp lipid metabolism, several lipid metabolism pathways closely related to hair loss and scalp oil problems in young women were identified using KEGG database enrichment analysis, including the sphingolipid metabolism pathway, neurotrophin signaling pathway, and ether lipid metabolism. The sphingolipid metabolism pathway is influenced by inflammatory mediators and key enzymes regulated by various stimuli, altering the relative abundance of metabolic molecules such as ceramides and sphingosine-1-phosphate (S1P), which can affect the hair follicle environment and hair growth cycle.

The effects of PFP on superoxide dismutase (SOD) and β-galactosidase (SA-β-Gal) were studied using a dihydrotestosterone (DHT)-stimulated human dermal papilla cell model. Cytotoxicity assays indicated that PFP concentrations below 0.0625 % (m/V) were non-toxic to dermal papilla cells. Compared to the BC group, the SOD activity of the DHT-stimulated NC group was significantly decreased ($p < 0.01$), confirming successful model establishment. The SOD improvement rates of PFP at 0.0313%, 0.0625%, and 0.1250% (m/V) were 31.12%, 35.64%, and 41.41%, respectively. The improvement rates of SA-β-Gal were 15.36%, 39.86% and 48.87%, respectively. These results indicate that PFP possesses antioxidant properties, potentially removing harmful free radicals by increasing SOD activity, inhibiting age-related markers of hair follicle stem cells, and delaying hair follicle atrophy, thereby exerting anti-hair loss effects.

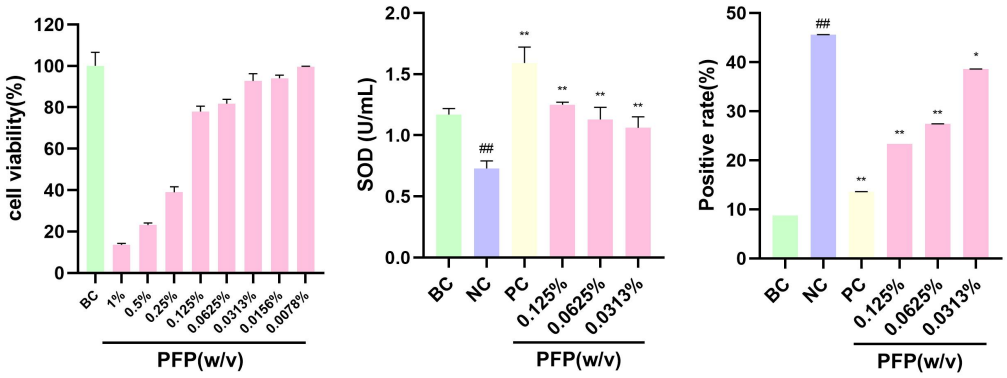

Figure 8. Regulatory effect of PFP on alopecia-related targets.

4 Conclusions

This study comprehensively demonstrated the significant anti-aging and scalp rejuvenation effects of PFP through a combination of in vitro experiments, scalp metabolomics, and the analysis of key physiological parameters related to female pattern hair loss. By comparing differences in scalp physiological indicators, lipid metabolism, and the scalp microenvironment, the study revealed potential underlying causes of hair loss and oily scalp conditions in young women. These factors included excessive scalp sebum secretion, alterations in the local scalp environment, disruptions in sebum metabolism, and regional variations in scalp characteristics. The interactions among these factors may collectively influence the hair growth cycle and overall scalp health in this demographic.

PFP exerted beneficial effects through multiple mechanisms, including the inhibition of elastase and MMP-1 activity, promotion of skin cell repair and collagen production, enhancement of hyaluronic acid and chondroitin sulfate levels, regulation of scalp lipid and microbial metabolism, suppression of β-galactosidase activity, and stimulation of vascular endothelial growth factor (VEGF) expression. These diverse actions contribute to improvements in both skin and scalp health.

In summary, PFP show promising potential as active ingredients in future anti-aging and scalp care formulations. Their multifaceted biological properties provide novel, natural-based solutions for addressing the challenges of cutaneous and scalp aging as well as hair loss, making them valuable candidates for applications in the cosmetic and dermatological industries. However, this study was primarily based on in vitro experiments and scalp physiological analyses within a specific population, which may limit the generalizability of the findings. Therefore, future studies involving large-scale clinical trials and diverse populations are warranted to further validate the efficacy and safety of PFP and to explore their underlying mechanisms of action in skin and scalp care.

Acknowledgements

NONE.

References

[1] ZHANG F, QU J, THAKUR K, et al. Purification and identification of an antioxidative peptide from peony (Paeonia suffruticosa Andr.) seed dreg [J]. Food chemistry, 2019, 285: 266-74.
[2] LV M, YANG Y, CHOISY P, et al. Flavonoid components and anti-photoaging activity of flower extracts from six Paeonia cultivars [J]. Industrial Crops and Products, 2023, 200: 116707.
[3] BIRCH M, MESSENGER J, MESSENGER A. Hair density, hair diameter and the prevalence of female pattern hair loss [J]. British Journal of Dermatology, 2001, 144(2): 297-304.
[4] SNYDER F. Ether-linked lipids and their bioactive species: Occurrence, chemistry, metabolism, regulation, and function [M]. New Comprehensive Biochemistry. Elsevier. 1996: 183-210.
[5] CHYLIŃSKA N, MACIEJCZYK M. Hyaluronic Acid and Skin: Its Role in Aging and Wound-Healing Processes [J]. Gels, 2025, 11(4): 281.
[6] HURTADO M M, ZENG X, VAN DER HEIDE E. The human skin and hydration [M]. Hydrated Materials. Jenny Stanford Publishing. 2015: 51-80.
[7] MENON G, KLIGMAN A. Barrier functions of human skin: a holistic view [J]. Skin pharmacology and physiology, 2009, 22(4): 178-89.
[8] TRüEB R M. Oxidative stress and its impact on skin, scalp and hair [J]. International journal of cosmetic science, 2021, 43: S9-S13.